

Solvent interaction with the (2p3s) Rydberg state of hexamethylenetetramine: Energetics and relaxation dynamics

Q. Y. Shang, C. Dion, and E. R. Bernstein

Citation: *The Journal of Chemical Physics* **101**, 118 (1994); doi: 10.1063/1.468494

View online: <http://dx.doi.org/10.1063/1.468494>

View Table of Contents: <http://aip.scitation.org/toc/jcp/101/1>

Published by the *American Institute of Physics*

COMPLETELY

REDESIGNED!



**PHYSICS
TODAY**

Physics Today Buyer's Guide
Search with a purpose.

Solvent interaction with the (2p3s) Rydberg state of hexamethylenetetramine: Energetics and relaxation dynamics

Q. Y. Shang, C. Dion, and E. R. Bernstein

Department of Chemistry, Colorado State University, Fort Collins, Colorado 80523

(Received 23 November 1993; accepted 17 March 1994)

The (1+1) mass resolved excitation spectra are reported for the $(2p3s) \leftarrow (2p)^2$ Rydberg transition of the tricyclic, high symmetry molecule hexamethylenetetramine [HMT ($C_6H_{12}N_4$)] and its van der Waals clusters. The solvent molecules employed include both nonpolar (Ar, CH_4) and polar (NH_3 , CH_3OCH_3) species. HMT and its clusters are generated and cooled in a supersonic expansion. The observed electronic transition is assigned as $T_2 \leftarrow A_1$ within the T_d point group. A transition blue shift of 52 cm^{-1} for each Ar atom and 65 cm^{-1} for each methane molecule in the HMT van der Waals cluster is characterized. These shifts are caused by an excited state repulsive interaction between the excited Rydberg electron and the closed shell solvent which reduces the attractive dispersion interaction between the HMT and nonpolar solvent species in the van der Waals cluster. A transition red shift of more than 600 cm^{-1} for NH_3 and CH_3OCH_3 solvent/HMT clusters is observed; this large increase in interaction energy for the excited Rydberg state of HMT with respect to the ground state of HMT is associated with the delocalization of the excited electron into available (virtual) Rydberg orbitals of the solvent molecules. The interaction is characterized as an electron transfer interaction. These results and assignments are consistent with previously reported ones for DABCO/solvent clusters. Relaxation dynamics of excited HMT and its clusters are investigated via a pump/probe (ionization) technique. Relaxation of the clusters is dominated by an intersystem crossing mechanism resulting in an excited state singlet lifetime of $\sim 5 \text{ ns}$ compared to a bare molecule HMT excited state lifetime of $\sim 1.0 \mu\text{s}$. A triplet state of HMT lies 255 cm^{-1} below the first excited singlet Rydberg state as determined by two-color threshold ionization studies.

I. INTRODUCTION

The effects of solute/solvent interactions in $(2p3s)$ Rydberg electronic states of azabicyclo(2.2.2)octane [$C_7H_{13}N$, (ABCO)] and diazabicyclo(2.2.2)octane [$C_6H_{12}N_2$, (DABCO)] have recently been characterized.¹⁻³ Depending on the solvent electronic and electrical properties, three different types of interactions are proposed to account for the transition energies and dynamics of the clusters. A Pauli exclusion principle (or exchange repulsive) interaction between the excited Rydberg electron ($3s$) and the closed shell of rare gas atoms and nonpolar molecules contributes (negatively) to the overall dispersive attractive potential to generate a cluster transition blue shift with respect to the bare molecule Rydberg transition. The cluster is thus less tightly bound in the $(2p3s)$ Rydberg state than in the ground state. An attractive dipole/induced dipole interaction can add to the dispersion and fermion repulsion to enhance the overall attractive interaction in the Rydberg state. Depending on relative sizes of the various contributions, these components can account for either red or blue shifted cluster transitions. If the solvent molecule has available virtual Rydberg orbitals at comparable $(2p3s)$ energies, then an electron transfer interaction, a sharing of the Rydberg excited electron between the solute and solvent molecules, can contribute a very large attractive interaction to the overall solute/solvent binding energy in the excited electronic state and thereby generate a very large ($\sim 600 \text{ cm}^{-1}$) cluster transition red shift. These three interactions are especially pronounced for Rydberg electronic states because of the diffuseness and delocalization of the excited Rydberg orbitals. The interactions also manifest themselves

in the cluster Rydberg state dynamics. Intersystem crossing and electron transfer reduce the observed lifetimes of these van der Waals clusters by as much as a factor of 10.⁴

In order to demonstrate the generality of such cluster interactions and dynamics for Rydberg states, we have studied the properties and behavior of other molecules in van der Waals clusters using $(2+1)$ -resonance enhanced multiphoton ionization for a number of alkanes and ethers.⁵⁻⁷ With the notable exception of dioxane, most $(2+1)$ -mass resolved excitation spectra are too weak to observe a wide variety of cluster systems and states. Amines, on the other hand, typically have low lying $(2p3s) \leftarrow (2p)^2$ Rydberg transitions that are accessible to $(1+1)$ -mass resolved excitation spectroscopy and which are therefore much more intense. A wide variety of cluster spectra for such amines are much more readily obtained. In this paper, we report the study of one such amine/cluster system—hexamethylenetetramine [(HMT, $C_6H_{12}N_4$)] solvated by nonpolar and polar species.

HMT has an adamantane cage structure with four CH groups replaced by four nitrogen atoms. Each chair-like ring in HMT contains three symmetrically distributed N atoms. The electronic energy levels of this cage structure are not well understood or explored.⁸ The $(2p3s) \leftarrow (2p)^2$ Rydberg transition is expected to be the lowest energy transition since all amines thus far studied have this property.⁹ Only broad two-photon spectra have been previously reported for this molecule.

II. EXPERIMENTAL PROCEDURES

Our supersonic jet/time of flight mass spectrometer has been previously described with regard to this appli-

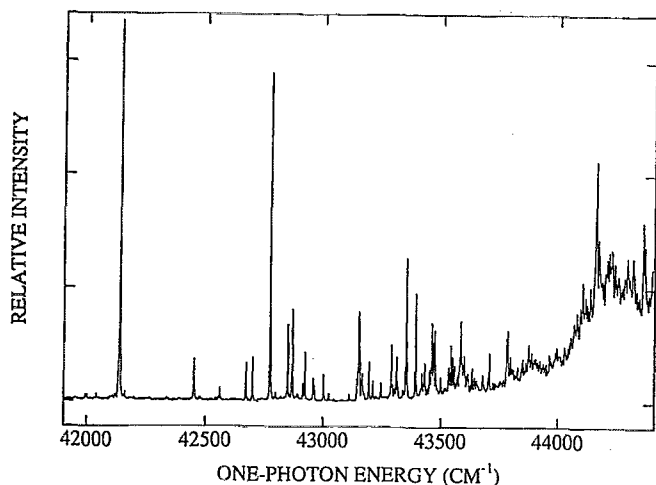


FIG. 1. The (1+1) one-color mass resolved excitation spectrum of HMT. The origin lies at 42 140 cm^{-1} . The transition is assigned as $(2p3s) \leftarrow (2p)^2(T_2 \leftarrow A_1)$.

cation.^{3,5,10} HMT is purchased from Aldrich Chemical Co., placed in a pulsed nozzle and heated to $\sim 150^\circ\text{C}$. The sample is cooled by a He expansion at 50 psi backing pressure, and solvent vapor is mixed into the expansion gas at $\sim 1\%$ pressure. Excitation and ionization are effected by two Nd/YAG pumped dye lasers. The dye solutions for excitation contain one of the following dyes: DCM, R640, Kiton red, R610, and R590. The fundamental dye output is doubled and subsequently mixed with 1064 nm YAG fundamental light. The ionization laser contains coumarin dyes C440, C460, or C480. The excited state lifetime is measured by a pump/probe technique as described previously.⁴ The main variation of this technique for the present application relates to the wide range (~ 5 ns to 1 μs) in excited state measured lifetimes. For the bare molecule (long lifetime), the lasers must intersect the beam at somewhat different positions as described in Ref. 4.

III. RESULTS

A. The (1+1)-mass resolved excitation spectrum (MRES) of HMT

The one-color (1+1) MRES of HMT is displayed in Fig. 1. The ion signal is at the HMT parent mass channel. The intense feature at 42 141 cm^{-1} is assigned as the $(2p3s) \leftarrow (2p)^2$ Rydberg transition origin. Many vibronic features are observed in this spectrum and they are tabulated in Table I. The excitation spectrum at energies in excess of 44 500 cm^{-1} is increasingly intense and broad. This latter absorption is probably due to another electronic transition. The features displayed in Fig. 1, many of which are weak, are the only sharp ones in this spectral region.

B. HMT/Ar geometry

Upon supersonic cooling, HMT forms clusters with many different solvents; the solute/solvent clusters are typically formed in the minimum energy configurations. The possible minimum energy cluster geometries are calculated

TABLE I. List of observed peaks in the mass resolved one-photon excitation spectrum of HMT.

Observed transition (cm^{-1})	Vibrational energy (cm^{-1})	Intensity ^a	Assignments ^b
42 141		s	Origin
42 455	314	m	
42 563	422	w	
42 674	533	m	
42 701	560	m	
42 777	636	s	$\nu_4(799)$
42 851	710	m	
42 871	730	m	
42 916	775	w	
42 926	785	w	
42 960	819	w	
42 963	822	w	
43 005	864	w	
43 026	885	vw	
43 112	971	vw	
43 144	1003	w	
43 152	1011	m	$\nu_3(1048)$
43 154	1013	w	
43 167	1026	w	
43 198	1057	w	
43 213	1072	w	
43 248	1107	w	
43 292	1151	m	
43 297	1156	vw	
43 315	1174	w	
43 321	1180	vw	
43 341	1200	vw	
43 357	1216	m	
43 395	1254	m	$2 \times 636(2\nu_4)$
43 422	1281	w	
43 433	1292	w	
43 455	1315	w	
43 463	1322	m	
43 473	1332	m	
43 480	1339	vw	
43 500	1359	w	
43 535	1394	w	
43 543	1402	w	
43 550	1409	w	
43 558	1417	vw	
43 585	1444	m	$\nu_2(1469)$
43 598	1457	w	
43 633	1492	vw	
43 678	1537	vw	
43 707	1566	w	
43 780	1639	w	
43 785	1644	w	$636 + 1011(\nu_4 + \nu_3)$
43 795	1654	vw	
43 827	1686	vw	
43 849	1708	vw	
43 874	1733	w	
43 887	1746	vw	
44 105	1964	vw	
44 161	2020	vw	$2 \times 1011(2\nu_3)$
44 172	2031	w	
44 360	2219	w	
44 482	2341	w	

^as—strong; m—medium strong; w—weak; vw—very weak.

^bThe number in parentheses is the ground state vibrational frequency.

with a classical atom-atom interaction potential employing a Lennard-Jones-Coulomb potential and MOPAC 6.0¹¹ calculated HMT geometry and atomic charges (corrected for

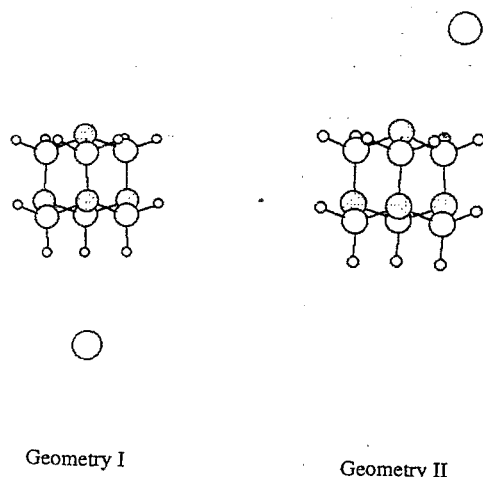


FIG. 2. Two minimum energy geometries of $\text{HMT}(\text{Ar})_1$ calculated from a Lennard-Jones potential energy function. The binding energy is $\sim 300 \text{ cm}^{-1}/\text{Ar}$ independent of cluster size. The $\text{HMT}(\text{CH}_4)_1$ clusters have the same conformations and the binding energies are both $\sim 400 \text{ cm}^{-1}$ in the ground state.

known systemic inaccuracy).¹ Two geometries are obtained for the $\text{HMT}(\text{Ar})_1$ cluster and these are shown in Fig. 2. Geometry I has an argon atom above a cyclohexane ring on its threefold axis. The binding energy in the ground electronic state for this cluster is 289 cm^{-1} . The HMT molecule has four such equivalent sites. Geometry II has an argon atom located near a nitrogen atom at a low symmetry site (off the threefold axis). The binding energy for this cluster is 308 cm^{-1} . The HMT molecule has 12 such equivalent sites. These two sites are very similar to those calculated for dioxane,⁵ DABCO, and ABCO/Ar clusters.¹ $\text{HMT}(\text{CH}_4)_1$ has the same set of two sites with a ground state binding energy of $\sim 400 \text{ cm}^{-1}$.

C. The (1+1) MRES of HMT/nonpolar solvent clusters

1. HMT/Ar

Figure 3 shows the (1+1) MRES monitored in the $\text{HMT}(\text{Ar})_1$ and $\text{HMT}(\text{Ar})_2$ mass channels. Signals in higher order cluster mass channels are vanishingly small. The first peak in the $\text{HMT}(\text{Ar})_1$ mass channel appears at $42\,192 \text{ cm}^{-1}$, blue shifted 52 cm^{-1} from the bare molecule 0_0^0 transition. An additional feature with about one-half the intensity of the latter peak appears at $42\,208 \text{ cm}^{-1}$, 15 cm^{-1} further to high energy. Additionally two weak features are found at $42\,244$ and $42\,257 \text{ cm}^{-1}$ in this MRES. No other significant features are identified in this spectrum.

The first peak in the spectrum obtained by monitoring the $\text{HMT}(\text{Ar})_2$ mass channel lies at $42\,244 \text{ cm}^{-1}$; it is shifted to the blue of the HMT bare molecule origin by 104 cm^{-1} ($2 \times 52 \text{ cm}^{-1}$). The second feature (at about one-half the intensity of the first) is 13 cm^{-1} further to the blue ($42\,257 \text{ cm}^{-1}$). Three additional features can be identified in this spectrum: a broad one at $\sim 42\,297 \text{ cm}^{-1}$ and two others at $42\,559$ and $42\,611 \text{ cm}^{-1}$.

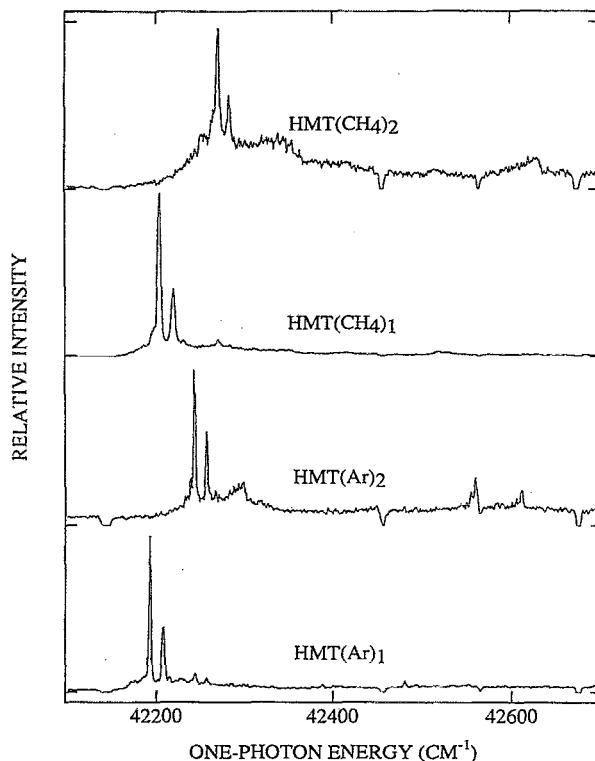


FIG. 3. The (1+1) one-color mass resolved excitation spectra monitored in the mass channel of $\text{HMT}(\text{Ar})_1$, $\text{HMT}(\text{Ar})_2$, $\text{HMT}(\text{CH}_4)_1$, and $\text{HMT}(\text{CH}_4)_2$, respectively. The negative signal is due to detector saturation by a strong bare molecule peak signal.

The fact that the blue shifts of 0_0^0 transition for $\text{HMT}(\text{Ar})_1$ and $(\text{Ar})_2$ clusters are 52 and 104 cm^{-1} , respectively, suggests that the argon atoms reside in these clusters at equivalent sites. The second peak in these spectra are 15 and 13 cm^{-1} , respectively, to the higher energy side of each origin. This is typical for a van der Waals vibrational mode, although the assignment is not certain at this time. Additionally, one can observe the $\text{HMT}(\text{Ar})_2$ features in the $\text{HMT}(\text{Ar})_1$ mass channel ($42\,244$ and $42\,257 \text{ cm}^{-1}$); this suggests that the $\text{HMT}(\text{Ar})_2^+$ cluster dissociates upon formation in this one-color experiment. The broad feature at $42\,297 \text{ cm}^{-1}$ in the $\text{HMT}(\text{Ar})_2$ mass channel spectrum is due to dissociation from the $\text{HMT}(\text{Ar})_3$ cluster. This cluster transition is blue shifted $\sim 52 \text{ cm}^{-1}$ from that of $\text{HMT}(\text{Ar})_2$. One concludes that even for $\text{HMT}(\text{Ar})_3$, all the solvent argon atoms occupy the same type site on the HMT molecule.

The internal mode at 315 cm^{-1} from the 0_0^0 transition is observed for the $\text{HMT}(\text{Ar})_2$ cluster, but not the $\text{HMT}(\text{Ar})_1$ cluster. Recall that the binding energy for $\text{HMT}(\text{Ar})_1$ in the excited state is only 237 cm^{-1} [$(289-52) \text{ cm}^{-1}$] and thus the cluster can readily dissociate if the vibrational energy gets into the van der Waals modes.¹² For $\text{HMT}(\text{Ar})_2$, the dissociation is slower because more modes are available to distribute the vibrational energy. Vibrational redistribution must be relatively rapid in this system.¹²

Two geometries (Fig. 2) are calculated for the $\text{HMT}(\text{Ar})_1$ cluster; however, only one cluster geometry appears to be present in the expansion. Considering the results for

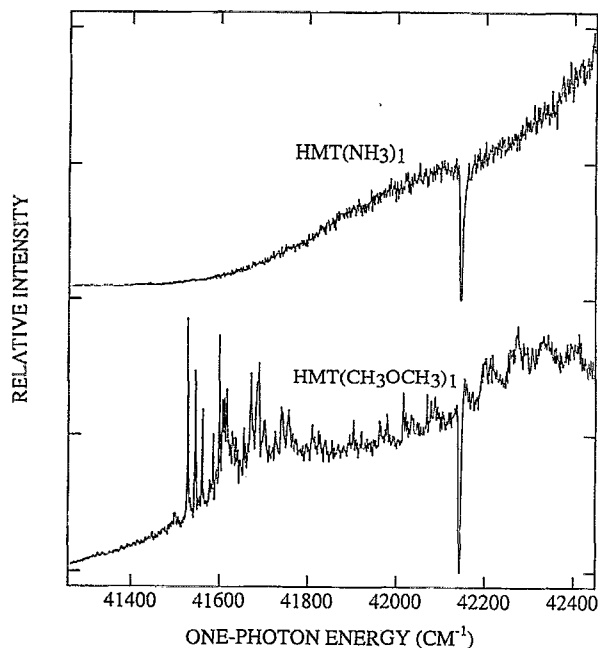


FIG. 4. The (1+1) one-color mass resolved excitation spectra monitored in the mass channel of $\text{HMT}(\text{CH}_3\text{OCH}_3)_1$ and $\text{HMT}(\text{NH}_3)_1$, respectively. The negative signal is due to detector saturation by a strong bare molecule peak signal.

$\text{HMT}(\text{Ar})_1$, $\text{DABCO}(\text{Ar})_1$, and $\text{ABCO}(\text{Ar})_1$ with respect to both calculated structures and spectral shifts, we suggest that the $\text{HMT}(\text{Ar})_1$ cluster observed has geometry I of Fig. 2. The second and third argon atoms for $\text{HMT}(\text{Ar})_{2,3}$ must also reside at the same symmetry site based on their respective spectral shift values. The absence of spectra that can be associated with cluster geometry II is somewhat surprising, although not unprecedented,² in light of the fact that the solute/solvent ground state binding energies for the two cluster geometries are so similar ($\sim 300 \text{ cm}^{-1}$). A cluster with geometry II is probably in the expansion, but its spectra may be broad and weak due to poor Franck-Condon overlap and an anticipated large spectral blue shift (reduced excited state binding energy for this structure).

2. HMT/CH_4

Figure 3 also displays the spectra of $\text{HMT}(\text{CH}_4)_{1,2}$ as observed in their respective mass channels. The first feature observed in the $\text{HMT}(\text{CH}_4)_1$ mass channel falls at $42\,205 \text{ cm}^{-1}$, 65 cm^{-1} blue shifted from HMT bare molecule origin; a second feature appears 14 cm^{-1} to the blue of the first cluster transition. Two additional weak features appear at $42\,272$ and $42\,283 \text{ cm}^{-1}$ in this spectrum.

This spectrum is very similar to that discussed above for the $\text{HMT}(\text{Ar})_1$ cluster. The first peak is assigned as the 0_0^0 transition of the $\text{HMT}(\text{CH}_4)_1$ cluster with geometry I; the second feature is due to a transition involving an excited state van der Waals mode added to the cluster (geometry I) 0_0^0 ; and the two weak peaks to the blue of these are associated with the $\text{HMT}(\text{CH}_4)_2$ cluster (geometry I) photodissociated in the ion $[\text{HMT}(\text{CH}_4)_2^+ \rightarrow \text{HMT}(\text{CH}_4)_1^+ + \text{CH}_4]$ because of one-color (1+1) ionization.

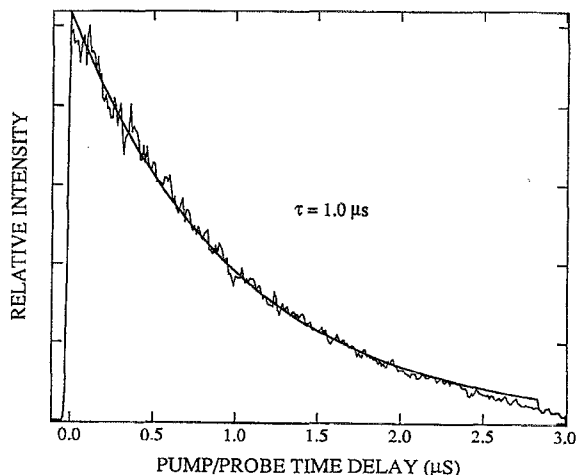


FIG. 5. Pump (excitation)/probe (ionization) lifetime decay of the ($2p3s$) excited singlet (1R_1) state of HMT at the origin. The ionization laser is at $22\,550 \text{ cm}^{-1}$. A single exponential function is used to fit the decay.

In the top spectrum of Fig. 3, we present the $\text{HMT}(\text{CH}_4)_2$ mass channel detected spectrum. The first feature at $42\,272 \text{ cm}^{-1}$ is 132 cm^{-1} blue shifted from the bare molecule HMT origin and the second feature ($42\,283 \text{ cm}^{-1}$) lies 14 cm^{-1} to the blue of it. Again these features are a cluster (geometry I) $\text{HMT}(\text{CH}_4)_2$ 0_0^0 transition and a van der Waals mode addition to it. The broad feature in this spectrum ($\sim 42\,320 \text{ cm}^{-1}$) is about 180 cm^{-1} blue shifted from the HMT 0_0^0 transition. Since this shift is close to $3 \times 65 \text{ cm}^{-1}$ (considering the width of the feature), we propose that it arises from $\text{HMT}(\text{CH}_4)_3$ fragmentation upon ionization.

D. HMT/polar solvent clusters

1. $\text{HMT}/\text{CH}_3\text{OCH}_3$

Figure 4 presents the spectrum monitored in the $\text{HMT}(\text{CH}_3\text{OCH}_3)_1$ for an expansion of the two species. Sharp peaks are observed at the onset of this spectrum, but they are built on a continuous and constantly rising background level throughout the spectral range accessed. Two-color, near threshold ionization did not change this appearance, and thus we suggest that the observed spectrum in the $\text{HMT}(\text{CH}_3\text{OCH}_3)_1$ mass channel is predominantly due to the $\text{HMT}(\text{CH}_3\text{OCH}_3)_1$ cluster. The spectrum is significantly red shifted from the HMT 0_0^0 transition; the first sharp feature at $41\,527 \text{ cm}^{-1}$ is -613 cm^{-1} from the HMT 0_0^0 at $42\,140 \text{ cm}^{-1}$. The sharp features following this 0_0^0 transition are due probably to van der Waals mode additions to the origin and possibly a cluster of another geometry.

2. HMT/NH_3

The spectrum of $\text{HMT}(\text{NH}_3)_1$ as shown in Figure 4 has no sharp features, but is also red shifted by more than 600 cm^{-1} from the bare molecule origin. This spectrum is not unlike that found for $\text{DABCO}(\text{NH}_3)_1$.³

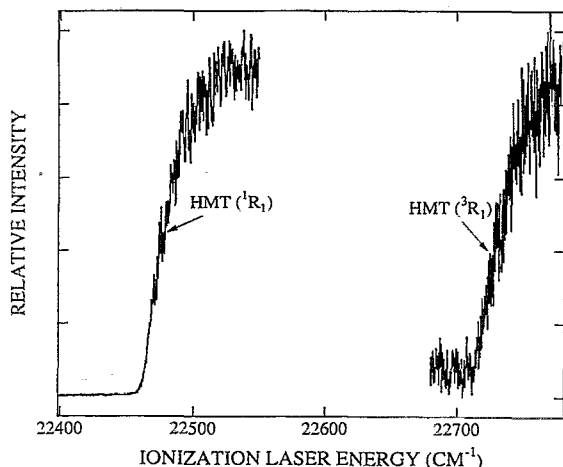


FIG. 6. The ionization threshold spectrum of HMT in the 1R_1 and 3R_x ($2p3s$) states. The singlet ($2p3s$) state is generated by exciting the HMT origin transition at $42\,140\text{ cm}^{-1}$. The triplet ($2p3s$) state is generated by exciting the $\text{HMT}(\text{Ar})_1$ cluster transition origin at $42\,192\text{ cm}^{-1}$, and monitoring the bare molecule mass channel after the ionization laser is delayed 20 ns with respect to the excitation laser.

E. Lifetime and ionization threshold

1. HMT bare molecule

Figure 5 presents the signal intensity in the HMT mass channel as a function of ionization laser (probe) delay time with respect to the excitation laser. The excitation energy is set at $42\,140\text{ cm}^{-1}$ to populate 0^0 and the ionization laser is set at $22\,550\text{ cm}^{-1}$. The decay is represented by a single exponential function with a decay time constant of $1.0\ \mu\text{s}$.

Figure 6 shows the ionization threshold for HMT. With the excitation laser tuned to the HMT 0^0 transition, the ionization threshold appears at $22\,460\text{ cm}^{-1}$.

2. HMT/solvent clusters

a. HMT(Ar)₁. The solid curve in Fig. 7 displays the signal intensity in the $\text{HMT}(\text{Ar})_1$ mass channel as a function of ionization laser delay time with respect to the excitation laser. The excitation laser energy is set at $42\,192\text{ cm}^{-1}$, the origin of the $\text{HMT}(\text{Ar})_1$ cluster Rydberg transition. The ionization laser energy is $22\,520\text{ cm}^{-1}$, slightly above that measured for the $\text{HMT}(\text{Ar})_1$ ionization threshold. The rise time represents the system (laser plus mass detector) resolution of

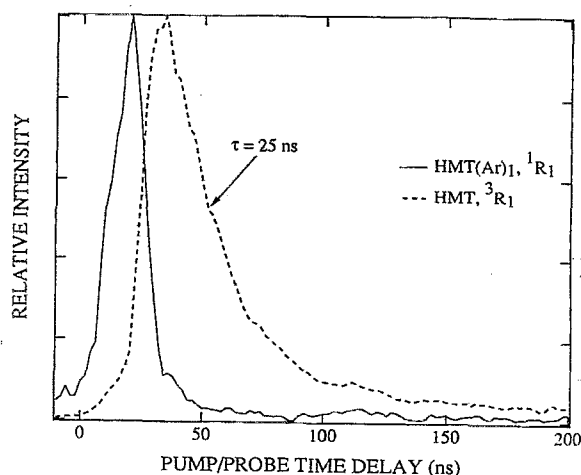
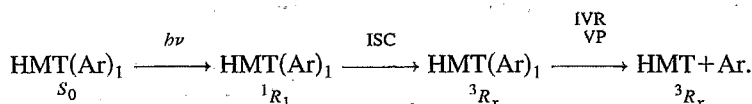


FIG. 7. Pump/probe lifetime decay of the signals in $\text{HMT}(\text{Ar})_1$ and HMT bare molecule mass channels. The excitation laser is at $42\,192\text{ cm}^{-1}$. The ionization laser is at $22\,520\text{ cm}^{-1}$ for $\text{HMT}(\text{Ar})_1$ and $22\,800\text{ cm}^{-1}$ for HMT. The decay curve for $\text{HMT}(\text{Ar})_1$ is instrument time resolution limited ($<10\text{ ns}$). A single exponential function is used to fit the decay in the HMT mass channel. The lifetime is $\sim 25\text{ ns}$.

$\sim 6\text{ ns}$. The decay of the $\text{HMT}(\text{Ar})_1$ first excited Rydberg singlet state [$(2p3s)^1R_1$] is clearly less than the instrument response function. Argon solvation of HMT has apparently shortened the HMT 1R_1 lifetime by nearly three orders of magnitude.

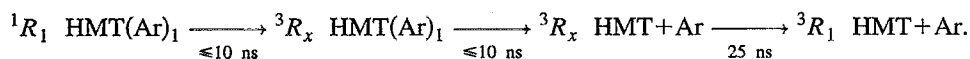
One can also observe the decay signal of the $\text{HMT}(\text{Ar})_1$ cluster in the bare HMT mass channel (see Fig. 7). The ionization energy used to detect this signal is $22\,800\text{ cm}^{-1}$; this energy is too small to fragment the cluster ion. The ionization threshold spectrum of this newly generated (from cluster vibrational predissociation) bare molecule is additionally displayed in Fig. 6. The cluster is excited to the $\text{HMT}(\text{Ar})_1 0^0$ transition, so no extra source of vibrational excitation of the cluster is available. As can be determined from Fig. 6, 255 cm^{-1} more energy is required to ionize the HMT produced from the dissociation of the cluster than is required to ionize the noncluster derived HMT molecule in 1R_1 . The conclusion must be that the cluster generated nascent HMT bare molecule product is in a triplet state (0^0 , probably), 255 cm^{-1} lower in energy than the 1R_1 state HMT. Similar behavior has been characterized and assigned for $\text{DABCO}(\text{Ar})_1$ as follows:^{3,4}



The $0^0\ ^1R_1$ $\text{HMT}(\text{Ar})_1$ cluster, following intersystem crossing (ISC), has 255 cm^{-1} of vibrational energy in the van der Waals modes (probably) and thus undergoes vibrational predissociation (VP). If the ISC generates internal vibrational modes of HMT, then intracuster vibrational energy redistribution (IVR) would occur prior to VP. These processes would probably occur on the 10^{-9} s time scale.

What is different about this HMT/solvent system with regard to others discussed previously⁴ is that the 3R_x state is so short lived ($\sim 25\text{ ns}$ for the decay curve of Fig. 7). One would expect a 3R_1 lifetime of roughly 10^{-3} s . A possible explanation for this short lifetime is that 3R_x is not the lowest HMT triplet state. We have not explored the nascent HMT ionization threshold

beyond 500 cm^{-1} higher in ionization energy. If the 3R_1 state were populated eventually in this system, a long lifetime excited triplet HMT molecule should be detected with sufficiently high ionization energy. Thus the overall dynamics of the system may be



Note finally that the new HMT bare molecule signal is delayed from the cluster signal by roughly 10 ns.

b. HMT(CH₄)₁. Figure 8 shows the decay of HMT(CH₄)₁ in the excited state. The excitation laser energy is $42\,205\text{ cm}^{-1}$ as required to excite the ${}^1R_1\ 0_0^0$ level of HMT(CH₄)₁. The behavior is quite similar to that displayed for HMT(Ar)₁ in Fig. 7. The decay constant is 25 ns for this cluster 1R_1 state. We suggest that the HMT(Ar)₁ and (CH₄)₁ clusters are governed by the same mechanistic behavior; nonetheless, a new HMT signal is not observed in the bare molecule mass channel following cluster signal decay. Since the cluster binding energy is 334 cm^{-1} in the excited 1R_1 state and the 3R_x state is only 255 cm^{-1} below the 1R_1 state, ISC ${}^1R_1 \rightarrow {}^3R_x$ would not provide enough energy to fragment the cluster. Further relaxation by internal conversion (IC) from 3R_x to 3R_1 might provide enough energy to fragment the cluster. If IC does subsequently occur to generate 3R_1 ionization laser may not be at high enough energy to generate the HMT ion ($I \leftarrow {}^3R_1$).

c. HMT(CH₃OCH₃)₁. Figure 8 also presents the decay signal for the HMT(CH₃OCH₃)₁ cluster when excited with $41\,527\text{ cm}^{-1}$ at its 0_0^0 transition and ionized with $22\,500\text{ cm}^{-1}$ laser radiation. Again a very short 25 ns lifetime is determined, which must be characteristic of the cluster ISC and IC dynamics. No bare molecule mass channel signal which follows the cluster decay can be observed. In the case of DABCO(CH₃OCH₃)₁, a constant signal is observed following a $0.2\ \mu\text{s}$ decay.

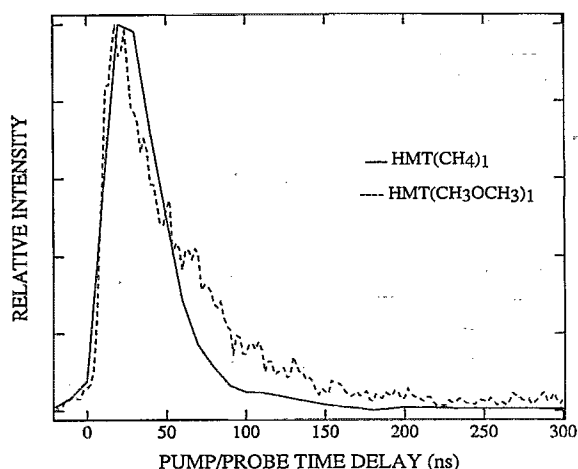


FIG. 8. Pump/probe lifetime decay of the signals in HMT(CH₄)₁ and HMT(CH₃OCH₃)₁ mass channels. The excitation laser is at $42\,205\text{ cm}^{-1}$ for HMT(CH₄)₁ and $41\,527\text{ cm}^{-1}$ for HMT(CH₃OCH₃)₁. The ionization laser is at $22\,500\text{ cm}^{-1}$. A single exponential function is used to fit the decays. Both clusters have $\sim 25\text{ ns}$ decay times.

IV. DISCUSSION

A. Transition assignment for HMT

HMT has a rigid adamantane-like structure. The ground state symmetry for HMT is T_d . The observed transition is assigned as a Rydberg state based on the blue shift of its Ar and CH₄ cluster spectra. The transition 0_0^0 lies at $42\,140\text{ cm}^{-1}$ and its ionization threshold energy is $22\,460\text{ cm}^{-1}$. This ionization threshold energy or term value is typical for a $3s$ terminating orbital for an amine. The total ionization energy ($I \leftarrow S_0$) is $64\,600\text{ cm}^{-1}$, this value is very close to the onset ionization of the photoelectron spectrum of the molecule.¹³ This spectrum is associated with a triply degenerate $t_2(2p)$ orbital.¹³ Thus, from the transition blue shift, term value, and total ionization energy, we assign the transition as $3s(a_1) \leftarrow 2p(t_2)$ with overall electronic symmetry $T_2 \leftarrow A_1$.

The $T_2 \leftarrow A_1$ transition is both one- and two-photon allowed. The observed cluster blue shift for each Ar and CH₄ solvent species in the cluster supports the 0_0^0 assignment. A second much more intense broad, one-photon allowed transition lies only a few thousand wave numbers to higher energy.

Ground state vibrational analysis¹⁴ shows that only four totally symmetric modes exist for HMT— $779(\nu_4)$, $1048(\nu_3)$, $1469(\nu_2)$, and $2883(\nu_1)\text{ cm}^{-1}$. We have assigned the three intense peaks to the first three totally symmetric modes 636 , 1011 , and 1444 cm^{-1} based on the close ${}^1R_1/S_0$ energy match (see Table I). Many more features are found in the spectrum that cannot be accounted for in this manner. A similar situation arises for the $(\sigma 3s) \leftarrow (\sigma)^2$ transition of adamantane.⁷ Features due to e, t_1, t_2 vibrations can appear in the spectrum and e and t_2 vibrations can be Jahn–Teller active.¹⁵

B. Solvent interaction with the HMT ($2p3s$) Rydberg state

The difference in energy between a transition for the bare chromophore and the transition for a cluster represents the interaction energy difference between the ground and excited state cluster. One can also think of this shift as due to the difference in ground and excited state cluster binding energy. These two conceptualizations for the transition shift are most useful and appropriate if the transition Franck–Condon factors (intensity distribution) are the same for both bare molecule and cluster. For HMT(Ar)₁ and HMT(CH₄)₁, the shifts are 52 and 65 cm^{-1} , respectively. These results compare well with those found for DABCO, ABCO/Ar, and CH₄ clusters for which the solvation site is found to be over the cyclohexane ring.^{1,2} This coincides with geometry I of Fig. 2. Four such sites are available for HMT. Geometry II

for these clusters (Fig. 2) should, in comparison, have a much larger cluster shift; it is not observed in these spectra. We did not observe sharp features for geometry II DABCO(CH₄)₁ clusters, due probably to Franck-Condon overlap (weak features) and broad features.

This cluster transition blue shift for nonpolar solvent molecules clustering with HMT (and DABCO, ABCO) is attributed to a repulsive interaction of the excited Rydberg state with the solvents. This repulsive component of the solute/solvent interaction arises from the expansion of the HMT electron density upon electronic excitation toward the closed shell solvent. This expansion generates a repulsion associated with the Pauli exclusion principle. The overall shift (repulsion) is smaller for HMT than for DABCO or ABCO because of either the larger HMT molecule polarizability (more red shift) or the different HMT Rydberg state electronic distribution.

The cluster transitions are red shifted by more than 600 cm⁻¹ for HMT/NH₃, CH₃OCH₃ systems. Again, the system behavior is comparable to that found for DABCO/amine and ether clusters³ in general, and NH₃ and CH₃OCH₃ clusters in particular, and we suggest the same interpretation for these HMT clusters. In this instance of strong excited state interaction between solute and solvent, the Rydberg electron delocalizes into the virtual, equienergetic orbitals of the solvent molecules. The cluster red shift is thus due to a large solute (HMT)-solvent (amines, ethers) electron transfer interaction. The 3s Rydberg orbitals for amines, ethers, HMT, DABCO, and ABCO are all at comparable energies.

C. Solvent induced relaxation of the (2p3s) Rydberg singlet state ¹R₁

The lifetime of the (2p3s)¹R₁ excited state of HMT is 1.0 μs. The long lifetime is related to the weakness of the transition and the decoupling of the ¹R₁ state from both valence and other Rydberg states. When HMT is clustered with Ar or CH₄, the excited ¹R₁ state HMT lifetime drops from 1.0 μs to 6 or 25 ns, respectively. This excited state lifetime reduction is attributed to enhanced intersystem crossing (ISC) in the cluster because the bare molecule is generated with this time constant and this newly generated HMT (from cluster dissociation) has an increased ionization energy compared to that of the ¹R₁ HMT generated by monomer optical excitation. The ISC results in an increase of 255 cm⁻¹ in ionization energy. The large increase in intersystem crossing and concomitant decrease in the lifetime of ¹R₁ could be due both to symmetry reduction and an external heavy atom effect. This gain in 255 cm⁻¹ of vibration energy in the triplet state is sufficient to generate the bare molecule due to dissociation of the cluster. The triplet lifetime is so surprisingly short (25 ns) perhaps because the triplet accessed by ISC is not the lowest triplet state and the employed ionization laser energy is insufficient to ionize the ³R₁ state eventually generated (25 ns) through (³R_x → ³R₁) internal conversion.

A comparable lifetime reduction is identified for HMT/CH₄, NH₃, CH₃OCH₃ clusters, but in these instances, the excited state cluster binding energy is large enough such that HMT molecule is not generated upon ISC. Additionally,

the lower triplet state may have enough excess vibrational energy to dissociate the cluster, but the ionization laser energy is too low to generate the I ← ³R₁ transition.

For DABCO/amine and ether clusters, a full electron transfer reaction final product state could be identified. In HMT/amine and ether clusters, the ISC rate is faster than the electron transfer rate and thus the triplet states are generated before the electron transfer state. The electron transfer state could be generated from the triplet state of amine and ether clusters. As is the case for DABCO,^{3,4} the generation of the electron transfer state must be relatively slow (~100 ns) due to an activation energy or barrier probably generated by electronic potential energy surface couplings and geometrical changes along the reaction coordinate. We have previously argued that the ³R_x - ¹R_x energy differences are small due to reduced exchange coupling between these electronic configurations.^{3,4} An electron transfer state could be observed with a pump/probe ionization experiment if the probe ionization energy were sufficient and the ionization cross section were large.⁴

In summary, the relaxation dynamic of the HMT cluster is dominated by very rapid ISC most likely activated by symmetry reduction upon cluster formation. The nacent triplet state for the ISC may not be ³R₁, but a higher one, possibly related to a valence excitation. The red shifts observed for polar ether and amine clusters are dominated by an electron transfer interaction and the blue shifts for nonpolar solvents are dominated by a Pauli exclusion principle interaction.

V. CONCLUSION

The (1+1)-mass resolved excitation spectra of HMT and its clusters with polar and nonpolar solvents are reported. The transition is assigned as a (2p3s) ← (2p)² T₂ ← A₁ symmetry (T_d group) Rydberg excitation with the HMT 0₀⁰ transition at 42 141 cm⁻¹ and a term value (ionization energy, I ← ¹R₁) of 22 460 cm⁻¹. Both totally symmetric and nontotally symmetric vibronic transitions are observed in this T₂ ← A₁ electronic excitation.

HMT clusters with Ar, CH₄, NH₃, and CH₃OCH₃ are also studied. A solvent number additive blue shift is observed for this transition in argon clusters [52 cm⁻¹ (Ar)] and in CH₄ clusters [65 cm⁻¹/(CH₄).] The blue shifts are due to repulsive Pauli exclusion interaction terms between the 3s Rydberg electron and the closed shells of the solvent. A more than 600 cm⁻¹ red shift is found for the HMT transition in polar solvent clusters. The dominant red shift is due to delocalization or electron transfer of the 3s HMT electron into the comparable virtual orbitals of amine and ether solvents. These results are very similar to those found for similar DABCO clusters.

The relaxation of HMT and its solvent clusters in the (2p3s) Rydberg state is also investigated with a pump/probe mass selective ionization technique. The HMT ¹R₁ state has a long lifetime (1.0 μs); however, when clustered with any solvent, even argon, this excited lifetime ¹R₁ is dramatically reduced to less than 5 ns. The reduced cluster ¹R₁ lifetime is caused by an enhanced intersystem crossing to equal energy triplet state levels. Two cluster effects could generate this

enhanced ISC—an external heavy atom effect which causes the HMT/Ar clusters to have a shorter lifetime than the other clusters, and a reduction in HMT symmetry which would affect all HMT clusters more or less equally. This generated cluster triplet state has a high enough vibrational excitation (255 cm^{-1}) to dissociate the argon cluster and generate 3R_x HMT. The 3R_x HMT has a lifetime of roughly 25 ns and probably decays to 3R_1 which is not ionized in these experiments. The HMT(CH₄)₁ cluster 3R_x also decays in 25 ns to the same lower triplet state, but does not generate 3R_x HMT bare molecule because the cluster binding energy is too large. HMT polar solvent clusters also undergo ISC to 3R_x and 3R_1 and probably a charge transfer state, but neither of the latter two states are ionized (detected) in these experiments. The behavior characterized for HMT closely parallels that observed for DABCO, suggesting that the interactions and dynamics characterized for ($2p3s$) Rydberg states are quite general.

ACKNOWLEDGMENT

This effort is supported by the U.S. Army Research Office.

- ¹Q. Y. Shang, P. O. Moreno, S. Li, and E. R. Bernstein, *J. Chem. Phys.* **98**, 1876 (1993).
- ²Q. Y. Shang, P. O. Moreno, C. Dion, and E. R. Bernstein, *J. Chem. Phys.* **98**, 6769 (1993).
- ³Q. Y. Shang, P. O. Moreno, and E. R. Bernstein, *J. Am. Chem. Soc.* **116**, 302 (1994).
- ⁴Q. Y. Shang, P. O. Moreno, and E. R. Bernstein, *J. Am. Chem. Soc.* **116**, 311 (1994).
- ⁵P. O. Moreno, Q. Y. Shang, and E. R. Bernstein, *J. Chem. Phys.* **97**, 2869 (1992).
- ⁶Q. Y. Shang, P. O. Moreno, R. Disselkamp, and E. R. Bernstein, *J. Chem. Phys.* **98**, 3703 (1993).
- ⁷Q. Y. Shang and E. R. Bernstein, *J. Chem. Phys.* **100**, 8625 (1994).
- ⁸B. A. Heath, W. A. Kuebler, and M. B. Robin, *J. Chem. Phys.* **70**, 3362 (1979).
- ⁹M. B. Robin, *Higher Excited States of Polyatomic Molecules* (Academic, New York, 1974), Vol. 1.
- ¹⁰K. Law, M. Schauer, and E. R. Bernstein, *J. Chem. Phys.* **80**, 207 (1984).
- ¹¹J. J. P. Stewart, *A General Molecular Orbital Package*, 6th ed, QCPE No. 455, 1989.
- ¹²M. F. Hineman, S. Kim, E. R. Bernstein, and D. F. Kelley, *J. Chem. Phys.* **96**, 4904 (1992).
- ¹³W. Schmidt, *Tetrahedron* **29**, 2129 (1973).
- ¹⁴G. Dolling, G. S. Pawley, and B. M. Powell, *Proc. R. Soc. London Ser. A* **333**, 363 (1973).
- ¹⁵G. Herzberg, *Electronic Spectra and Electronic Structure of Polyatomic Molecules* (Van Nostrand Reinhold, New York, 1966).